Superconducting Nanowire Detectors for the EIC

A proposal for EIC-Related Generic Detector R&D

Submitted July 14, 2023

PI: Whitney Armstrong (warmstrong@anl.gov)
Contact Person: Sangbaek Lee (sangbaek.lee@anl.gov)

Whitney Armstrong, Sylvester Joosten, Sangbaek Lee, Zein-Eddine Meziani, Valentine Novosad, Chao Peng, Tomas Polakovic, Shivangi Prasad, Marshall Scott, Junqi Xie, Maria Żurek

Argonne National Laboratory

Davide Braga, Farah Fahim, Adam Quinn, Kyle Woodworth

Fermi National Accelerator Laboratory

Karl Berggren, Alessandro Buzzi, Matteo Castellani, Reed Foster, Owen Medeiros

Massachusetts Institute of Technology

Matthew Shaw

JPL

Dave Gaskell, Ben Raydo, Holly Szumila-Vance

Jefferson Lab

Abstract

Owing to their unparalleled timing resolution and quantum efficiency, superconducting nanowire single photon detectors (SNSPDs) have become the dominant technology in quantum optics. SNSPDs can operate with excellent detection efficiency at high rates in magnetic fields above $5\,\mathrm{T}$ with near zero dark count rate. Efforts are underway to develop low power cryoCMOS readout ASICs with novel superconducting electronics as a hybrid cryogenic detector readout architecture. Because nanowires are a relatively new technology in the fields of nuclear and particle physics, the proposed R&D program will investigate the radiation hardness of superconducting nanowire sensors, superconducting electronics, and a prototype cryoCMOS front-end readout ASIC. We will test the performance of these devices while operating in a high background radiation environment. We will also investigate the radiation hardness of superconducting devices exposed to an intense source of electron, neutron, and gamma radiation to identify modes of failure for sensors, which otherwise, are anticipated to be quite radiation hard. We also reported on our progress as this proposal was awarded in FY22.

Contents

1 Proposal

1.1 Introduction

Superconducting nanowire single photon detectors (SNSPD) have, since their initial discovery [1], found many applications in fields of nanophotonics and quantum communication. Metrics like sub-20 ps timing jitter [2], nearly 100% quantum efficiency up to IR wavelengths [3, 4] and count rates as high as 10^9 counts/s with effectively zero dark counts [5] make them the go-to choice in many applications, including LIDAR systems [6], quantum teleportation [7], quantum key distribution [8], optical quantum computing [9], and many others [10]. Many, if not all, of these applications leverage the unique capability of detecting individual photons with unprecedented timing resolution and low noise.

We propose to develop superconducting nanowire detectors for applications at the Electron Ion Collider. The targeted R&D will focus on investigating the operational limits in high radiation environments and quantify the dose needed to cause lasting damage to the operation of SNSPDs. This information will be important for designing detector systems at locations requiring radiation-hard pixel sensors, for example, in the far forward and backward regions at the EIC. The unique capability of SNSPDs to operate in high magnetic fields at cryogenic temperatures with excellent position and time resolution – combined with the proposed measurements verifying the anticipated high degree radiation hardness (see section 1.3.2 presents tremendous new opportunities for detector configurations incapable with current technologies. For example, integrating a superconducting nanowire tracking detector in the bore of a superconducting magnet in the forward ion region to detect particles otherwise lost into the magnets becomes possible once we understand the operational lifetime or failure rate in this configuration.

In section 1.2, we motivate the detector R&D with a discussion of some high-impact science enabled by this new detector technology. Section 1.3 presents the design, construction, and theory of operation for SNSPDs and the hybrid cryogenic detector architecture under development. From a discussion of photon detection, we then shift to a brief review of their use as *particle* detectors, and conclude with a discussion of possible detector concepts for the EIC. Section 1.5 outlines the R&D plan to measure the radiation hardness of all components in the complete detector system, and identify R&D milestones and deliverables for the project. Finally, the requested budget is presented in section 1.6 along with a narrative for the various funding scenarios.

1.2 Motivation

With the Electron Ion Collider project well underway, numerous opportunities which leverage the capabilities of superconducting nanowire detectors to enhance the scientific program exist [11]. The EIC User's Group engaged in a community-wide effort to write the EIC Yellow Report [12] outlining the science requirements for detectors. A key detector requirement is 4π hermiticity. Here we emphasize the physics of the far forward hadron region where high energy hadrons with little transverse momentum need to be detected. Challenges arise when instrumenting very close to the

ion beam, especially as the beam position and size vary as each ion bunch is accelerated. Also, holes in detector acceptance appear as the transition from forward detectors to the *far* forward region where a sequence of accelerator magnets are needed. Radiation damage, high magnetic fields, and cryogenic temperatures put constraints on location and space for detectors in this region where hermetic detection is ideal.

Motivating EIC Science Some of the big questions motivating the construction of an EIC were highlighted in a recent assessment from the National Academies of Sciences, Engineering, and Medicine [13]. These questions are:

- How does the mass of the nucleon arise?
- How does the spin of the nucleon arise?
- What are the emergent properties of dense systems of gluons?

The world's first polarized electron and polarized ion collider aims to address these questions. Furthermore, a large number of deep exclusive and semi-inclusive processes will be measured at the EIC, forming the hadron tomography experimental program which aims to produce 3D images (or distributions) of polarized quarks and gluons in nucleons and nuclei. The far forward detector requirements for the science outlined in the white paper [11] have been presented in a previous EIC R&D proposal to develop Roman Pot detectors [14]. Here we build on this motivation and discuss some important physics mentioned in the recently published yellow report [12].

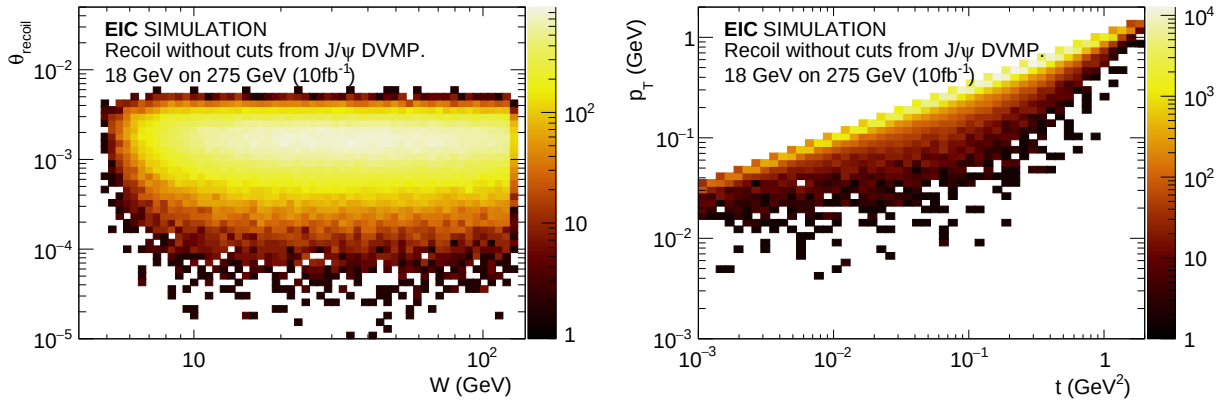

Figure 1: Recoil kinematics for J/ψ production at a high-energy EIC configuration. The left panel shows the recoil angle (in radians) as a function of W, while the right panel shows the recoil p_T as a function of the Mandelstam variable t.

Origin of the Proton Mass Protons and neutrons are responsible for 99% of the mass of the visible universe. Modern calculations indicate that the proton mass is dynamical in origin and

almost entirely unaffected by the value of the quark mass. The origin of the nucleon's mass is a hot topic in nuclear science, highlighted in the 2015 Long Range Plan for Nuclear Science : "*The vast majority [...] is due to quantum fluctuations of quark-antiquark pairs, the gluons and the energy associated with quarks moving around close to the speed of light*". Furthermore, the 2018 NAS report for the EIC identified the origin of the nucleon mass as one of the most important profound questions to be addressed at an EIC.

The proton mass is intimately related to the trace anomaly of the QCD energy-momentum tensor, experimentally accessible through the quarkonium (J/ψ and Υ) photo-production cross section near threshold. Alternatively, the trace anomaly can also be accessed through the interference between J/ψ photo-production and Bethe-Heitler pair production near the J/ψ threshold.

Far-forward recoil acceptance will be critical to maximize the potential program of this fundamental program at the EIC. Figure 1 shows the recoil kinematics at a higher-energy EIC configuration. The recoil proton is restricted to very small angles. Small angle/low p_T acceptance will be particularly important to measure the differential production cross sections for events with $t \sim t_{\text{min}}$.

Tomography of Nuclei The nuclear tomography program at the EIC will reveal the 3-dimensional quark and gluon structure of nuclear matter. Unraveling this information involves measuring multiple fully exclusive hard scattering processes to extract the generalized parton distributions (GPDs) [15]. The quark and gluon GPDs encode a position space tomographic image of hadronic matter, and measuring these processes is a significant part of the scientific program at Jefferson Lab and for the EIC.

The most prominent exclusive process involving GPDs is deeply virtual Compton scattering (DVCS). At EIC kinematics, the reaction $p(e, e'\gamma p)$ requires measuring a forward scattered proton in addition to the scattered electron and electro-produced photon. In the case of DVCS on the proton, the typical momentum transfers cause the proton to scatter at intermediate to small angles, which will be detected by a forward detector or far forward detector.

In addition to protons, the nuclear tomography program is also interested in studying light and medium nuclei. For example, coherent DVCS on ^{4}He has been recently measured [16] and is the subject of a group of upcoming experiments at JLab [17]. However, for collider kinematics at fixed momentum transfer, as the mass of the nucleus increases the scattered angle becomes smaller. Measuring these ions at very small angles is quite difficult and is often done in a Roman pot type configuration 10s of meters downstream of the interaction point. Because of the extremely small angle, and small momentum transfer relative to the ion beam energy, the recoiling ion is nearly indistinguishable from the unperturbed ion beam.

Other Processes Other processes requiring far forward detection were identified [18]. Charged current $e - p$ cross-sections and asymmetries will need detection pushed as far forward as possible to extract important quantities like the polarized sea quark distributions and the high-x $\bar{s}$ distribution. Also, for Jets and Heavy Flavor physics, forward detection and displaced vertex resolution is important for the open heavy flavor measurements at the EIC.

1.3 Superconducting Nanowire Sensors

1.3.1 Photon Detectors

A superconducting nanowire detector is a microelectronic device that utilizes critical phenomena in superconductivity to transform energy or heat into an electrical signal. Typical realization of a nanowire detector pixel can be seen in Figure 2: The sensitive area (usually on the order of 20×20 $\mu\mathrm{m}^2$) is covered by a densely packed superconducting nanostrip with a cross-section of roughly 10×100 nm^2 and a total length of approximately 1 mm. The narrow detecting wire is connected to wider superconducting leads that can connect it to other pixels or contact pads for a 2-wire electronic read-out which also doubles as the current supply. The sensitive area of the device can be increased by connecting multiple pixels in parallel. This increases the detection rate proportional to number of sub-pixels and decreasing signal by a factor inversely proportional to this number. As typical signals are usually on the order of $10\,\mathrm{mV}$, this is not a fundamental concern.

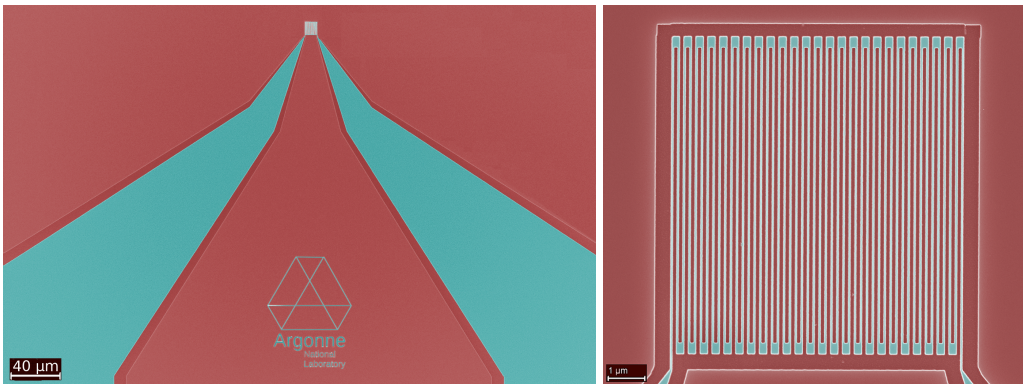

Figure 2: False color SEM micrograph showing a typical superconducting nanowire device developed at Argonne. The right image is closer view of the $10\,\mu\mathrm{m} \times 10\,\mu\mathrm{m}$ meandering nanowire geometry.

Nanowire Photon Detector Operation The detection process of a SNSPD can be divided into stages which are roughly sketched in Figure 3. First, a very thin and narrow nanowire is maintained well below the superconducting critical temperature T_C and is constant-current biased at current values close to critical currents (Figure 3a). Absorption of a single photon with energy $\hbar\omega$ much higher than the superconducting energy gap Δ, (i.e., $\hbar\omega \gg 2\Delta \approx 2\,\mathrm{meV}$), will lead to excitation of two quasi-electrons with high kinetic energies, and those will begin to inelastically scatter with other quasi-particles in the system. This forms the initial so-called hot spot [19] (Figure 3b). The approximate time-scales associated with this process are on the order of 10 ps [20] (dictated by the electron-phonon scattering times). The next stage of the detection process is the expansion of the hot spot (Figure 3c). First, the quasi-particles further multiply due to inelastic scattering and move diffusively outwards, towards the edges of the nanowire. The depletion of Cooper pairs leads to

local reduction of the order parameter and redistribution of the current in the region [21]. If the nanowire is biased close to critical currents, the current density in the hot spot region rises above the critical values and the superconducting state vanishes completely creating a normal state region that bisects the superconducting wire (Figure 3d). As the section of the wire turns normal, a voltage drop is generated across the wire and this voltage spike is registered as a resistance spike which corresponds to a single photon detection event. In the last stage, the current bias is reduced, either passively through a parallel resistive shunt, or actively using an electronically controlled current source and the hot spot shrinks and vanishes, preparing the nanowire for the next detection event (Figure 3e).

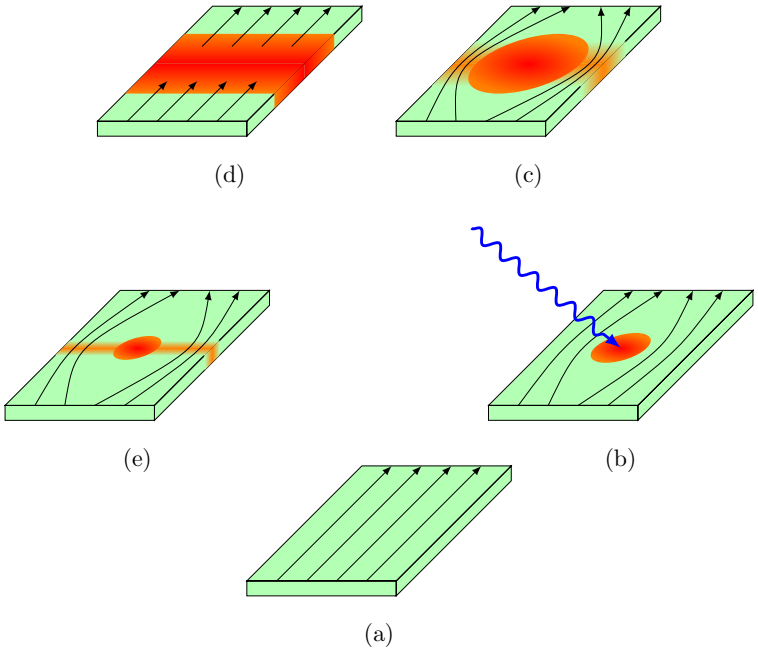

Figure 3: Schematic of the detection process through the hot spot formation after photon absorption. Equilibrium superconductor is in green, orange to red depicts regions with increasingly suppressed order parameter and black lines depict the superconducting current density. Blue arrow is a schematic depiction of an incoming single photon.

Through this process, a single particle, which would conventionally cause a signal well below the noise threshold, can cause a change of more than 6 orders of magnitude in the wire resistance. This dramatic change can be detected without any significant signal preconditioning or amplification. SNSPDs have been demonstrated to be superior in many figures of merit for photon detectors: timing resolution of less than 20 ps, a short reset time of approximately 10 ns, dark count rate of less than 10 counts/s/pixel, and a single photon resolution with more than 90% efficiency even at infra-red wavelengths [3].

The detection mechanism is based on a change of quantum mechanical correlation between electrons (i.e. breaking of Cooper pairs only eliminates the entangled two-electron state, not the

electrons themselves), which means that leaves the material unaltered by structural changes or changes to the single-electron system. This leads to longer detector lifetimes when compared to ionizing detectors, such as photomultiplier tubes and SiPMs, where redistribution of electronic densities during detection process generates strong electric fields and can cause irreversible microstructural defects.

Time Resolution Timing resolution is determined by the timing jitter of the device, which is the statistical variation of the time delay (typically reported as FWHM of the distribution). The variation has two contributions: an extrinsic variation due to the geometry of the wire, where there's a different time delay depending on where along the length of the wire the photon gets absorbed (in a typical meander geometry, the wire length can reach a few mm) and jitter associated with the timing of the read-out electronics [2]. Then there is the intrinsic variation that's due to the probabilistic nature of the processes that lead to the detection event. Typical values of timing jitter of SNSPD detectors are around 15 ps and are dominated by the noise jitter of the read-out [22], which can reduced down to 7 ps, a value due to geometric jitter [23]. On a short nano-bridge geometry, the intrinsic timing jitter of 2.7 ps [24] is reported, which is thought as the current fundamental limit to timing of the SNSPD devices.

High magnetic fields, low temperatures Typical experimental conditions of any collider experiment involve strong magnetic fields and often times cryogenic temperatures in close proximity to the superconducting beam line magnets. At cryogenic temperatures, charge carrier freeze-out depletes Si-based photomultipliers and causes serious performance degradation [25]. The presence of strong magnetic fields also leads to decrease of detection efficiency, especially when using photomultiplier tubes.

As SNSPDs are superconducting, operation in cryogenic environments below a sensor's T_c does not cause any degradation in their performance. Low-dimensional superconductors (such as superconducting nanowires) can persist in a Meissner state at fields higher than those for bulk superconductors. Significant effort was put towards developing technologies for scalable production of superconducting films that can sustain high magnetic fields [26]. The Argonne group demonstrated that superconducting nanowire detectors capable of high-rate, zero dark count detection in fields as high as 5 T [27], as shown in Figure 4, where the device operates with effectively zero dark count rate until the bias current is close to the field dependent I_c. While these field values should be sufficient for the EIC detector requirements, we believe that higher field operation can be achieved by geometrical optimization [28].

Radiation Hardness Performance in strong radiation fields is an open question, we do however believe that superconductors can be robust against radiation damage, as long as complex oxides (such as high-T_C superconducting cuprates) are avoided. This is especially true in the case of Niobium Nitride used for our devices because Nb has comparatively low neutron capture [29] and scattering [29, 30] cross-sections and the short electron screening length of the material [31, 32]

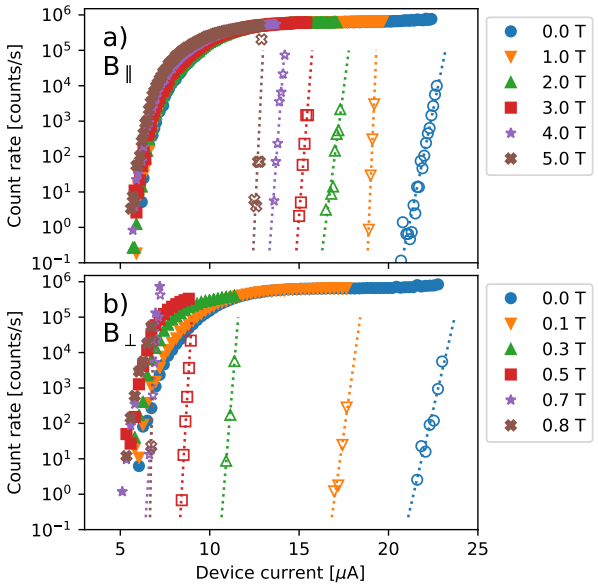

Figure 4: SNSPD bias current sweeps demonstrating performance at high fields (above: parallel, below: perpendicular) [27]. Full symbols indicate total count rate and empty symbols are dark counts. Notice that it is possible to find an operating point with zero dark counts and fully saturated detection efficiency.

makes it more robust against lattice defects. The Argonne group has exposed samples to a (poorly known) neutron flux by placing them near the beam dump of isotope separator (RAISOR) at the ATLAS facility at Argonne. After a few months they did not show any degradation of superconducting properties. The proposed R&D plan below aims to better quantify the dose using Argonne's LEAF user facility and to observe the onset of lattice defects from radiation damage. SNSPDs are anticipated to be significantly more radiation hard compared to silicon detectors, where neutron capture causes nuclear decay and doping of semiconductor devices leading to degraded performance and eventual failure.

1.3.2 Superconducting Nanowire Particle Detectors

Detection of energetic charged particles can be facilitated by two mechanisms. The first mechanism is scattering on the superconducting electrons directly, or indirectly through lattice phonons. The effect is no different from the photon absorption process – if the scattered particle deposits enough energy to break apart a Cooper pair, the excited quasi-particles will behave the same as those excited by photons.

The second mechanism is a thermal process [33]. In this thermal process, the hot spot in the nanowire is not created by diffusion and multiplication of quasi-particles, but by direct heat exchange with the microplasma in the particle track, creating a "hard" hot spot and completely

circumventing the need for the first two steps sketched in Figure 3.

Ion detection The concept of detecting low energy molecules has already found a limited use in high-performance time-of-flight mass spectrometry [34], particularly in the form micron-sized superconducting stripline detectors [35–38], which demonstrate that parallel superconducting wires provide both, high mass resolution and limited charge state discrimination of ions [39].

Low energy particle detection A previous study with radioactive sources [40] showed high detection efficiency of MeV α and β^- particles. An effort is underway at Argonne to understand the response of SNSPDs to different particles and to quantify how it may differ from the detection photons. Unlike the previous study using NbTiN nanowires which had a 30% background count correction, the Argonne group's SNSPDs have effectively zero dark count rate. Figure 5a shows a 4 SNSPD array where the wire width and spacing varies from $100\,\mathrm{nm}$ to $800\,\mathrm{nm}$. The preliminary results for the count rate Vs pixel size with a radioactive alpha source (^{241}Am) held at a fixed location in the cryostat is shown in Figure 5b, which appears to show a drop off in detection efficiency between $200\,\mathrm{nm}$ and $400\,\mathrm{nm}$. Similar results were also obtained with a beta source (^{90}Sr) and seem to indicate an optimum design for sensors with equal wire size and spacing. The ongoing work will also look at different wire geometries and incident particle angles and energies.

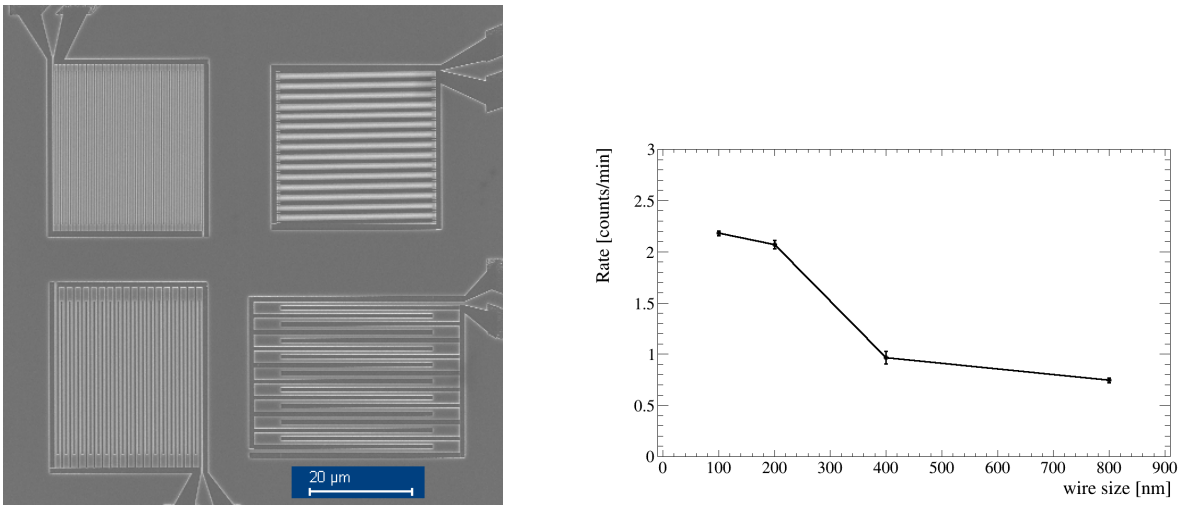

(a) (b)

Figure 5: SEM image (a) of a 4 pixel array where pixel's wire width and spacing are $100\,\mathrm{nm}$, $200\,\mathrm{nm}$, $400\,\mathrm{nm}$, and $800\,\mathrm{nm}$. Preliminary results for the count rate (b) from an ^{241}Am source held at a fixed location from the chip.

High energy particle detection In context of this proposal it is important to determine if SNSPDs are capable of detecting electrons at energies from a few hundred MeV up to 18 GeV and ions well

above 100 GeV. Detection of relativistic particles with SNSPDs has not been studied in literature, however, a 120 GeV proton will on average deposit 40 keV in $100\,\mu\mathrm{m}$ of silicon while a 1 MeV β will deposit roughly 15 keV in the same material. Given the high detection efficiency seen in β decays, along with the sub-eV detection of IR photons, SNSPDs will most likely detect high energy electrons and protons with high efficiency. Argonne has developed a cryogenic test bed for the Fermilab Test Beam Facility and has been working on testing with 120 GeV protons since January 2023.

Neutron detection Detection of charged particles is relatively straightforward because of comparatively high scattering cross-sections with the lattice and electrons of the superconductor and substrate. There might be, however, a desire to use SNSPDs to detect neutral particles such as neutrons. Working detection schemes utilizing SNSPDs are not yet developed but, for detection of neutrons, there exists a related technology that was used to demonstrate this capability: current biased kinetic inductance detectors (CBKID) [41–43] with a ^{10}B conversion layer.

In these devices a separate layer of ^{10}B is used [42, 43], or a more direct approach can be used when detectors were fabricated out of superconducting MgB_2 [44]. ^{10}B in the devices converts neutrons into energetic ^{4}He and ^{7}Li ions that are detected using a differential read-out of the CBKID delay line, which allows for a spatially-resolved measurement of neutron flux. Because the main neutron detection mechanism is through the conversion into charged particles, one can, in principle, substitute the CBKID devices with SNSPDs and construct a high-rate and high-speed detector of neutron flux with the same characteristics as discussed in the previous section.

1.4 State-of-the-art Instrumentation Opportunities at the EIC

Concept 1: Novel forward detectors Far forward detection is achieved with Roman pot detectors which are movable and share a vacuum with the beam pipe. Nanowire detectors will be thermally coupled to a 4 K cold-finger, and by operating within the beam-pipe vacuum, vacuum window material thickness is eliminated entirely. A windowless Roman pot detector, in combination with edgeless detection and (anticipated) high radiation hardness, provide an unmatched capability for extreme forward hadron detection. The so-called $10\ \sigma$ rule-of-thumb for Roman pots prevents the beam from damaging the detectors by limiting its proximity to the beam. Radiation hard nanowire detectors will be able to move closer to the beam, thus extending the acceptance reach at lower t.

The challenges for reading out a highly segmented cryogenic detector are similar to many other pixel detector technologies. The main difference here is the front-end read-out electronics operate at 4 K and send data over a high-speed serial connection as shown in Figure 6. This serial connection and a few power lines are then only connection required to operate and readout many detectors. Cryogenic read-out electronics have been successfully developed and operated at 4 K for applications in quantum computing [45]. Furthermore, a row/column readout reduces the number of channels from N^2 to $2N$ as was demonstrated in [46] and more recently with larger areas [47].

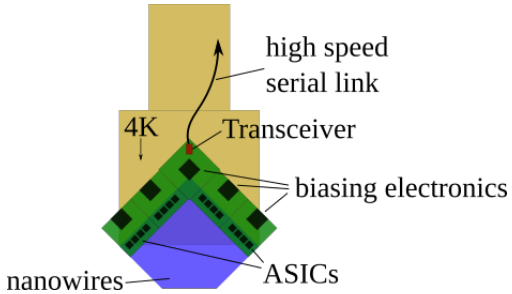

Figure 6: A cryogenic read-out scheme for a Roman pot superconducting nanowire detector. The front end electronics send the data over a high speed serial link with only a few wires leaving the cryostat.

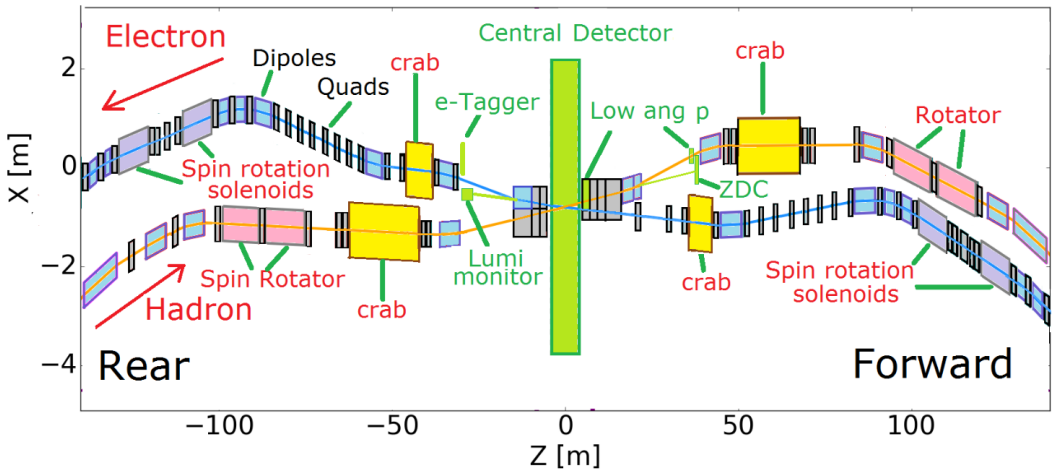

Figure 7: EIC IR with extended beam line magnets reproduced from the eRHIC design study [48].

Concept 2: Superconducting nanowire detector and superconducting magnet integration With many superconducting accelerator magnets at the EIC, there will be plenty of cooling power available from liquid helium, but in the forward B0 magnet region, there will be tight space constraints and many magnets before the first Roman pot station. These magnets introduce an acceptance hole due transitioning from the Forward (B0) region to the far forward Roman pot detectors. Therefore, integrating nanowire detectors with these superconducting magnets would create a more hermetic detector. This novel design would leverage the unique capabilities of the sensors to operate in strong magnetic fields at cryogenic temperatures to provide precision tracking and timing while sustaining operation in a high radiation environment. Such a new detection scheme could provide hermetic kinematic coverage in the forward hadron direction between the Roman pots, Zero-Degree Calorimeter (ZDC), and B0 spectrometer. Developing this concept necessarily involves EIC project engineers and physicists, but we must understand the radiation hardness of the detectors in context

of the lifetime of the EIC itself.

Concept 3: Neutral particle detector The forward hadron spectrometer has a large aperture to allow neutral particles to pass through to the ZDC shown in Figure 7. The ZDC will detect photons and neutrons with more demanding tracking requirements than previous detectors [49]. The small size, high radiation environment, close proximity to superconducting magnets, and particle tracking needs make it an attractive application for superconducting nanowire detectors. Instrumenting the front portion of the ZDC with a few cm^2 of tracking may dramatically improve performance with little modification to current designs. Similarly, the Compton polarimeter photon detector needs precise position reconstruction and a high resolution nanowire array with integrated superconducting logic can cut down background hits and identify the center of the shower in its early development.

Concept 4: Beam Loss Monitor Another possible application of nanowire sensors is as an auxiliary Beam Loss Monitor (BLM). The ion chambers are typically chosen for the BLM sensors for the modern accelerators like in RHIC [50] and CEBAF [51]. The nanowire can provide an extra, fast signal against the beam failure, thanks to the abundance of superconducting magnets that readily exists in the EIC beamline. The viability of the nanowire as a BLM should be demonstrated by the particle detection and radiation hardness tests discussed in section 1.5.

1.5 Research Plan

The proposed R&D project is composed of two parts, both addressing aspects of radiation hardness for components comprising a complete detector system for the EIC. In the first part, we propose to install a cryogenic test platform in Hall C (or A) where we will conduct opportunistic tests in parallel with the scheduled experiments. These tests will focus on the operational performance of (i) SNSPDs, (ii) superconducting electronics, and (iii) cryoCMOS ASICs in a high radiation environment. The second part of the proposed R&D consists of radiation hardness testing SNSPDs, superconducting electronics, and NbN thin films. This work will be conducted at Argonne's LEAF user facility. Devices and thin films will be irradiated by an intense 50 MeV electron beam at different doses and dose rates. We will look for the onset of lattice defects or other damage, as well as characterize the change in operating parameters (e.g. bias currents) of functioning devices. However, before discussing the proposed R&D plan, we first provide the background context of externally funded projects and on-going R&D.

1.5.1 Externally Funded R&D Efforts

There are a few ongoing research projects regarding cryogenic detectors and relevant areas. The Argonne group is continuing to investigate the performance of superconducting nanowires as particle detectors. Part of this work is the development of a cryogenic testbed located at the Fermilab Test

Beam Facility. We anticipate demonstrating high energy proton detection, an important milestone for the EIC. Since January 2023, when the beam time was the available, we have already taken . The details of measurement results are discussed in Section 4.1. At the last EIC Detector Advisory Committee Meeting reviewing new proposals, a small, yet symbolic amount of funding was allocated for eRD28: *Superconducting Nanowire Detectors for the EIC*. The committee noted in their recommendation, "Superconducting nanowires have never been deployed in a particle or nuclear physics experiment to our knowledge. As such, this proposal represents a true spirit of detector R&D [52]."

Microelectronics Co-Design Project A multi-institutional microelectronics co-design research project, *Hybrid Cryogenic Detector Architectures for Sensing and Edge Computing enabled by new Fabrication Processes* is addressing the need for a coherent yet adaptable approach to cryogenic readout systems. For a nice project overview, see this recent talk [53]. The project objectives are to advanced fabrication and integration techniques for cryogenic detectors, novel electronic readout and edge computing architectures, and readout electronics for integrated sensing and data reduction at source, through feature extraction and edge computing. In particular, the project will develop a hybrid architecture for cryogenic detectors, based on the co-design of superconducting sensor, novel superconducting electronics, and cryoCMOS readout ASIC in nanometer scale advanced processes. Figure 8 provides a conceptual overview of this project.

The MIT Quantum Nanostructures and Nanofabrication Group is developing and leading the superconducting electronics thrust of the project. The superconducting electronics will serve as an interfacing layer between the cyoCMOS ASIC and the nanowire sensors. These low power superconducting electronics use "x-Tron" based elements [54–57] and address the previous EIC Detector Advisory Committee concerns about power consumption and timing circuitry [52]. Additionally, this project aims to investigate the use of superconducting electronics to provide novel readout triggers and data reduction. A rough sketch of the overall readout scheme is shown in Figure 9.

The cryoCMOS ASIC thrust of this microelectronics project is being led by the Fermilab ASIC group. As the experts in fast electronics, they will develop a high channel count cryogenic CMOS readout ASICs to be bump-bonded to pixelated hybrid superconducting detectors. This again addresses the issue of power and scalable readout electronics, concerns expressed by the previous EIC Detector R&D Committee [52, 58].

1.5.2 High Radiation Environment Testing at JLab

We will take advantage of the EIC-like, high radiation environment found in JLab's Halls C. There a variety of liquid hydrogen and deuterium targets are used and provide typical luminosities on the order of $10^{37}\text{cm}^{-2}\text{s}^{-1}$. We will make use of existing instruments to monitor the radiation in Hall C while also making use of silicon detectors as witness of the accumulated dose near the cryostat. This will be cross calibrated with an absolute measurements using neutron dosimeters and opti-chromic rods to produce estimates of the accumulated dose and scaled neutron fluence.

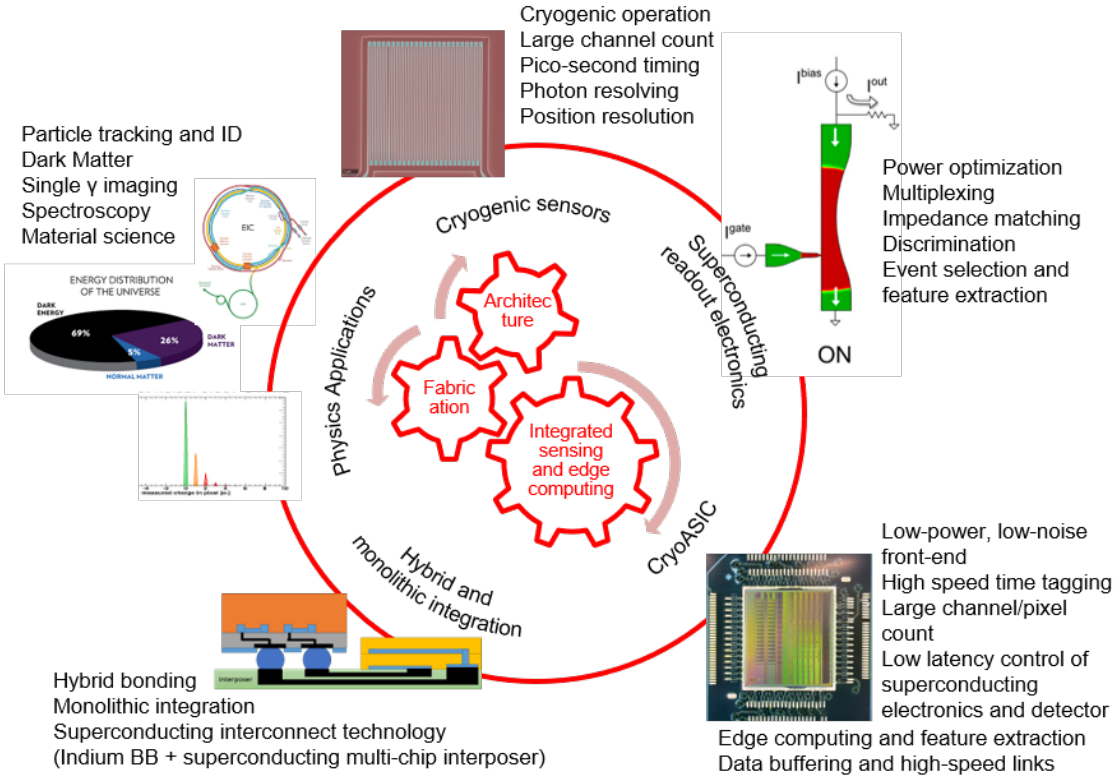

Figure 8: Conceptual illustration of the co-design framework underpinning the proposed microelectronics development.

Experimental Setup We request funds to purchase a new cryostat, such as the one shown in 10.. The cold head will be placed on a platform Hall C at beam height and $10\,\mathrm{m}$ Helium gas lines will connect to a water cooled compressor on the hall floor. This system will be highly movable as the cold head weighs roughly 60 lbs and is designed to sit on an optical table. The system also a small turbo pump station for a high vacuum system.

SNSPDs The SNSPDs tested will initially have the standard meander geometry, with a wire thickness of roughly 15 nm, wire width of 100 nm to 800 nm and similar spacing between wires. Basic pixel element will be $10 \times 10\ \mu\mathrm{m}^2$ (as shown in Figure 5-a). Larger-scale devices will be prepared by parallel connection of these units into larger single-channel super-pixels. The NbN thin films will be prepared by ion beam assisted sputtering as described in Refs. [26,27]. This process allows for a high quality thin film synthesis on 6" wafers and at room temperature. Initial devices will be fabricated on bulk Si or SiN substrates and performance of devices on suspended Si_3N_4 will be evaluated.

Fabricated devices will undergo standard characterization procedures with visible photons as described in our previous work [26, 27], including full characterisation of electronic and magnetic

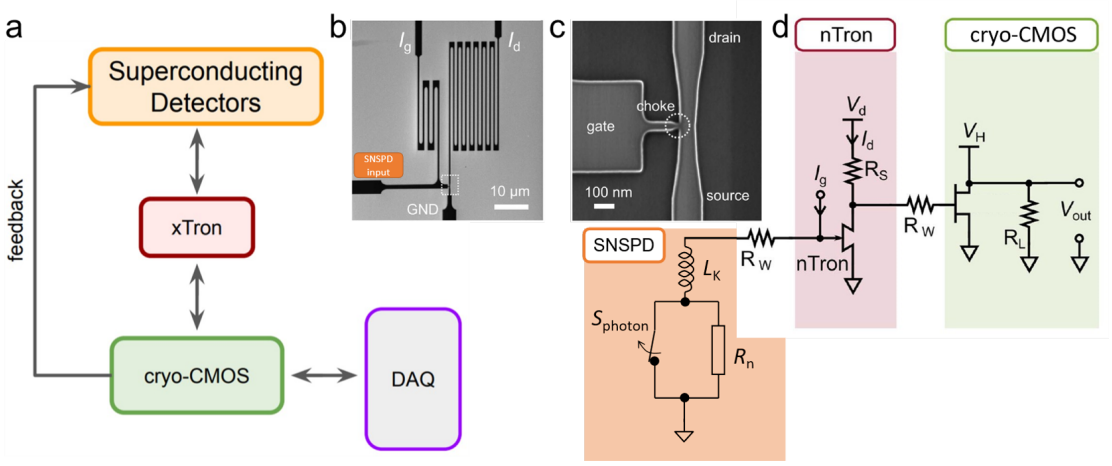

Figure 9: Hybrid sensing and edge computing architecture to be developed as part of the proposed program. (a) Schematic of system architecture. (b) SEM images of nTron comparator circuit with zoom-in showing nTron device itself. (d) Example of electrical schematic showing a fully integrated system based on SNSPD and nTron.

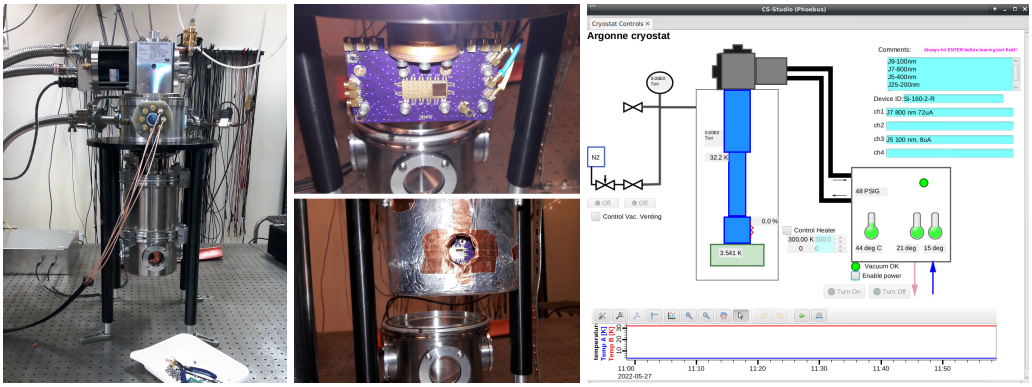

Figure 10: From left to right: Optical cryostat at Argonne (Helium compressor not shown), cold finger mounting stage PCB with mounted chip (top) and with shield installed (bottom), and EPICS based control system GUI.

properties of the parent material and transport properties of the finished device. After we confirm nominal operation with photons, particle detection performance will be checked with radioactive sources, to verify consistent detection characteristics for low energy charged particles.

We will begin by measuring the background rate as function running luminosity. A pulsed LED will determine the corresponding drop in detection efficiency high. This inefficiency is due to increased detector dead time as the background causes SNSPD to spend an increasing amount of time in the superconducting recovery stage (Figure 3e).

Superconducting Electronics The Quantum Nanostructures and Nanofabrication Group at MIT has agreed to supply a few superconducting nanowire binary shift registers [59] of various sizes. These devices will serve as a starting point for understanding how the element size effects their radiation tolerance of the basic building blocks for superconducting digital electronics [60], [61]. These results provide important insight as to where to focus future radiation hardening efforts, such as, triple modular redundancy, and under what conditions they are needed. Superconducting preamplifiers in the form of nTrons (see 9-c)will also test in this environment. We will investigate any changes observed between nTrons with various gate sizes and channel currents.

CryoCMOS ASICs Within the scope of a separate microelectronics R&D project titled "Hybrid Cryogenic Detector Architectures for Sensing and Edge Computing enabled by new Fabrication Processes" (HYDRA), Fermilab's ASIC group will soon produce a first prototype cryoCMOS ASICs for the readout of SNSPDs. After these are verified to operate as designed, we will test the operational performance of these as well. We look to quantify single event upset cross-section, displacement damage, and other cumulative damage relative to the established baseline performance at 4 K. These tests will the bit error cross-section using a built-in self test with > 20k registers used for sequential write and read operations looking for flipped bits. This will be done with external and shielded electronics developed at Fermilab.

1.5.3 Radiation Hardness testing at LEAF

The second major thrust of the proposed R&D consists of radiation hardness testing of superconducting devices. We will use standard SNSPDs and nTrons to study the damage and quantify the change in performance with accumulated dose, however, we are initially interested in establishing an upper limit for the accumulated dose on the NbN superconducting thin films. This is the limit where significant radiation damage accrues, defects form, and devices fail. This currently unknown limit will be critical for opening new applications at the EIC where access for maintenance is rare and the operational lifetime is on the scale of the EIC project as whole.

The Low-Energy Accelerator Facility (LEAF) at Argonne is a 50 MeV/25 kW electron linear accelerator primarily used to produce radioisotopes for medical, national security, basic science and industrial applications. The current budget requests funding for 1 week of operation, which will be spread over a series of 1 or 2 day runs. We will also coordinate with other experiments to conduct parasitic tests. The LEAF support staff will provide measurements and calculations of the particle fluences for each run.

Neutron dose The first run of tests will concentrate on high neutron fluence with the devices placed at 90 degrees relative to the high-Z converter. Devices will also be placed at smaller angles, exposing them to significantly more Bremsstrahlung.

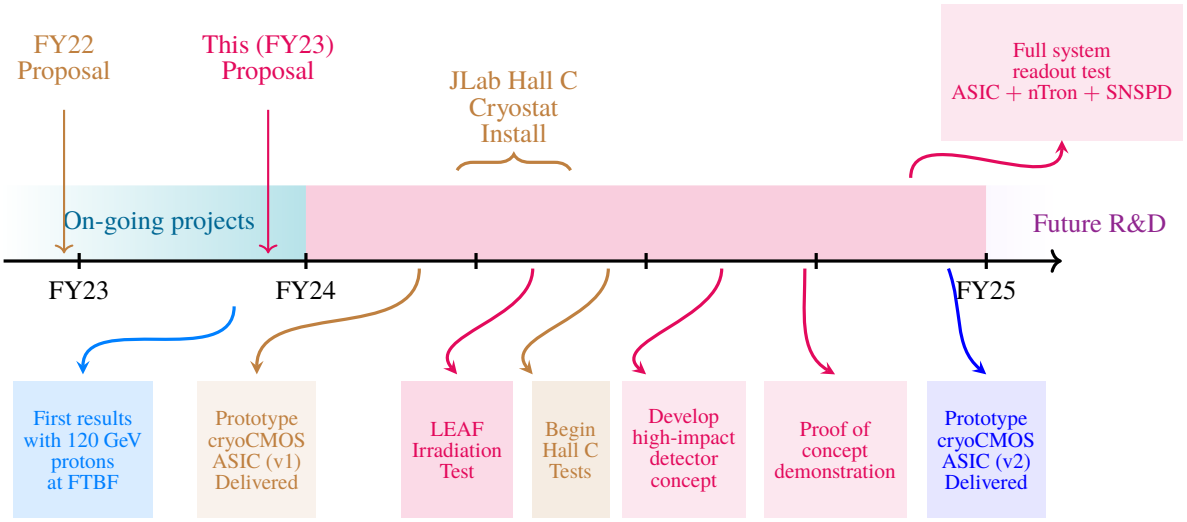

Figure 11: Timeline of proposed R&D projects for the FY23 cycle with some milestones from existing projects. Project milestones supported by FY22 and FY23 funding are color-coded in brown and red, respectively.

1.5.4 Project Milestones

The funding approved for the FY22 cycle should be practically used for the project performed in the FY23 cycle. Figure 11 shows synergy between other projects, FY22 funded projects and key milestones for the proposed R&D. The project milestones are color-coded differently for the FY22 R&D funding and FY23. It also shows a general strategy for developing a high-impact detector concept in subsequent years. The proposed milestones with schedule are:

1. Purchase a cryostat to be installed at JLab in Hall C (or A) — Aug. 2023
2. Prepare to operate the SNSPD with prototype cryoCMOS ASIC (v1) — Dec. 2023
3. Install cryostat at JLab in Hall C (or A) — Jan. 2024
4. Measure SNSPD background rate and dead time in high radiation environments.
   Measure the bit flip rate for the first prototype cryoCMOS ASIC in high radiation environments.
   Measure bit error rate for superconducting shift registers for a number of environments.
   - Run LEAF to irradiate SNSPDs at a various intensities and accumulated dose. — Feb. 2024
   - Begin to run JLab High Radiation Environment testing — Mar. 2024
5. Develop the design of the detector based on the sensors — May 2024
6. Test the full system of ASIC, nTron, shift register, and nanowire sensor — Sep. 2024

1.5.5 Deliverables

The deliverables of the project are as follows.

1. Radiation hardness of SNSPDs characterized with upper limit for the onset of defects and device failure.
2. Single Event upset cross-section for prototype cryoCMOS ASIC.
3. Background error rate for superconducting shift registers.
4. SNSPD efficiency in high radiation environment.

1.6 Budget

This project was awarded the EIC-Related Generic Detector R&D in FY22 cycle and access to funds only in June 2023. A budget of $138k that had been requested arrived to Argonne at its 80% level ($118k) at the end of June 2023. The money matrix and breakdown of budget for the previous proposal can be found in our FY22 proposal [62]. Given that we achieved 80% level funding, we reported our decision to delay the radiation hardness test at the LEAF to FY23 cycle at the Statement of Work (SoW). We will continue our efforts to establish a cryogenic testing platform and perfform the radiation hardness test at Jefferson Lab with the previously approved budget. The approved FNAL engineer support will be used for the ASIC's built-in self test structures.

In this updated proposal for FY23 cycle, we request $60k for the radiation hardness test at the LEAF. The institutional totals are shown in Table 1. Note that the travel support requested is for supporting collaboratiors for travel to radiation hardness tests at LEAF, Argonne National Laboratory, and Hall C (A), Jefferson Lab to diagnose the instruments and conduct measurements.

Table 1: Money matrix showing the totals associated with each institutional and task.

	Test at LEAF	Electronics	Travel Support	
Argonne National Laboratory	40k	10k	-	50k
All Institutions (ANL, FNAL, JPL, MIT, JLab)	-	-	10k	10k
	40k	10k	10k	

With the funding from FY23 cycle (October 1, 2023–September 30, 2024), we would like to focus on the radiation hardness testing at LEAF. The testing at LEAF (item 1) in mid-FY23 provides critical feedback about the limits of radiation hardness. We request for the budget for the electronics purchases needed for fabricating the bias board and ordering or soldering the micro coaxial cables. If completed in FY23, this detector project significantly advances feasibility and reduces the perceived risk for many applications ahead of the EIC project CD2/CD3a decision.

Table 2: Breakdown of individual budget items and the corresponding institutions.

Item No.	Description	Institution	Cost
1	One week of LEAF machine time	Argonne National Laboratory	40k
2	Purchase of Electronics	Argonne National Laboratory	10k
3	Travel	All	10k

A Realistic Nominal Budget (Baseline Budget) In this scenario, we perform the radiation hardness test at LEAF and Jefferson Lab as a priority. The nominal 1 week machine time at LEAF will be requested as planned.
Milestones

1. Perform the radiation hardness testing of the board at LEAF without operation of the sensor.
2. Verify the operation of the nanowire sensors at LEAF.
3. Perform the in-operando radiation hardness testing at LEAF.
4. Purchase ~ 10 bias boards for the nanowire sensor testing and the micro coaxial cables and connectors.
5. Test the full operation with shift registers, nTrons, and ASICs.

Nominal budget minus 20% In this scenario, we would cut LEAF facility run time from 1 week to 6 days. This would significantly reduce the range of exposures we can achieve. We would also reduce the purchase of electronics for bias board and cabling. This would likely delay the development of electronics needed for testing the various chips with different geometries, and the cryogenic logic with the nTrons and shift registers.

Milestones

1. Perform the radiation hardness testing of the board at LEAF without operation of the sensor (1 day.
2. Verify the operation of the nanowire sensors at LEAF.
3. If possible, perform the in-operando radiation hardness testing at LEAF.
4. Purchase ~ 3 bias boards for the nanowire sensor testing and the micro coaxial cables and connectors.

Nominal budget minus 40% - Under this scenario, we would cut LEAF facility run time from 1 week to 4 days. This would prevent design of new detector systems because the overall radiation hardness, and thus the detector lifetime, is less known. For example, magnet integrated nanowire sensors cannot begin in earnest because it requires time from project engineers that is hard to justify otherwise. We would also remove the purchase of electronics for bias board and cabling.

Milestones

1. Perform the radiation hardness testing of the board at LEAF without operation of the sensor.
2. If possible, verify the operation of the nanowire sensors at LEAF.
3. If possible, perform the in-operando radiation hardness testing at LEAF.

2 Cost Effectiveness

The nanowire sensors proposed in this document are typically made with 15 nm thick NbN layer on $8\,\mathrm{nm}\times 8\,\mathrm{nm}\times 300\,\mu\mathrm{m}$ thick silicon wafer. Thanks to its thin-film structure, the nanowire sensors are cost-effective and do not produce the significant amount of greenhouse gases. Fabrication facilities are readily available at Argonne National Laboratory's Materials Science Division and Center for Nanoscale Materials. This project will take advantage of existing user facilities such as the Fermilab Test Beam Facility and Jefferson Lab for testing purposes.

3 Diversity, Equity, and Inclusion

All participating institutions are committed to Diversity, Equity, and Inclusion. New ideas and opportunities are formed when respecting and valuing differences in race, gender, ethnicity, age, physical and language abilities, culture, religion, and sexual orientation. Approaches to problem-solving and decision-making are multi-dimensional, leading to success and empowering staff to thrive and do their best work.

4 Progress Report

This project was funded by the Generic EIC-related Detector R&D program in the FY22 cycle. We summarize the progress that have been made since the submission of the last proposal.

4.1 Detection of High Energy Protons

We tested the proton detection at the FTBF Meson Test Section 6.2 (MT6.2) enclosure with a a 120 GeV proton beam at the high rate about 10^6 per spill over 4.2 seconds. The NbN nanowire was installed inside the two-stage GM cryo-cooler based cryostat in the beam enclosure. The beam was

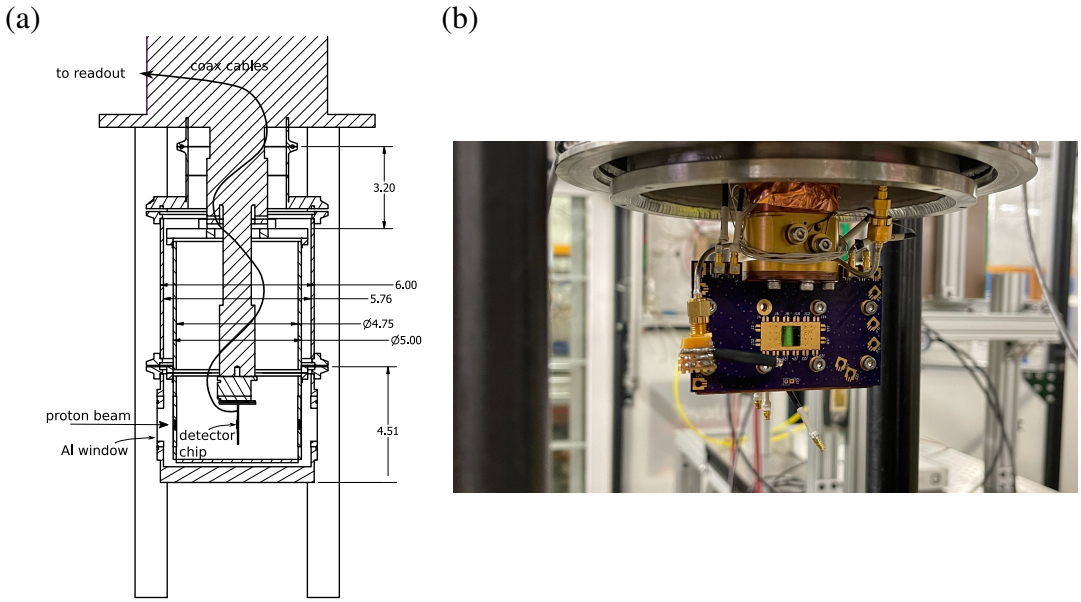

Figure 12: (a) A schematic drawing and (b) an image that illustrate the nanowire sensor enclosed inside the GM cryo-cooler based cryostat installed at the beam enclosure of FTBF MT 6.2.

incident on the sensor inside the cryostat as shown in Figure 12. The wires with widths of $300\,\mathrm{nm}$, $400\,\mathrm{nm}$, $600\,\mathrm{nm}$, and $800\,\mathrm{nm}$ were tested.

The proton incident on the sensor was identified as the electric signal from the nanowire sensor (Figure 13-a) in the presence of the proton signal from the auxillary plastic scintillators along the beamline (Figure 13-b). The timing coincidence between the nanowire signal and the scintillator allowed to measure the proton detection counts from the nanowire. Multi-wire Proportional Chambers (MWPCs) were used to determine the beam position and size [63]. Followed by the calibration runs to determine the optimal beam position that maximizes the proton counts, we took the production data that measures the proton count rate with respect to I_b/I_c, the bias current normalized to the critical current (Figure 13-c).

We have observed the competing effects in determining the optimal wire width. On one hand, the small width wires are advantageous because of the saturation of detection efficiency at smaller I_b/I_c, where the dark count rate is miniscule. On other hand, the smaller width wires have smaller critical current I_c, thus the smaller signal amplitude and the lower signal-to-noise ratio. This suggests that the optimal wire width for the proton detection to be around 200 nm, to be tested at the Fermilab Test Beam Facility after the summer 2023 shutdown.

4.2 Detection of Low Energy Alpha Particles

After the low energy α particle detection study mentioned in section 1.3.2 done with 0.1 μCi, we performed the bias scan test with 10 μCi ^{241}Am source that arrived in October 2022. The testbed

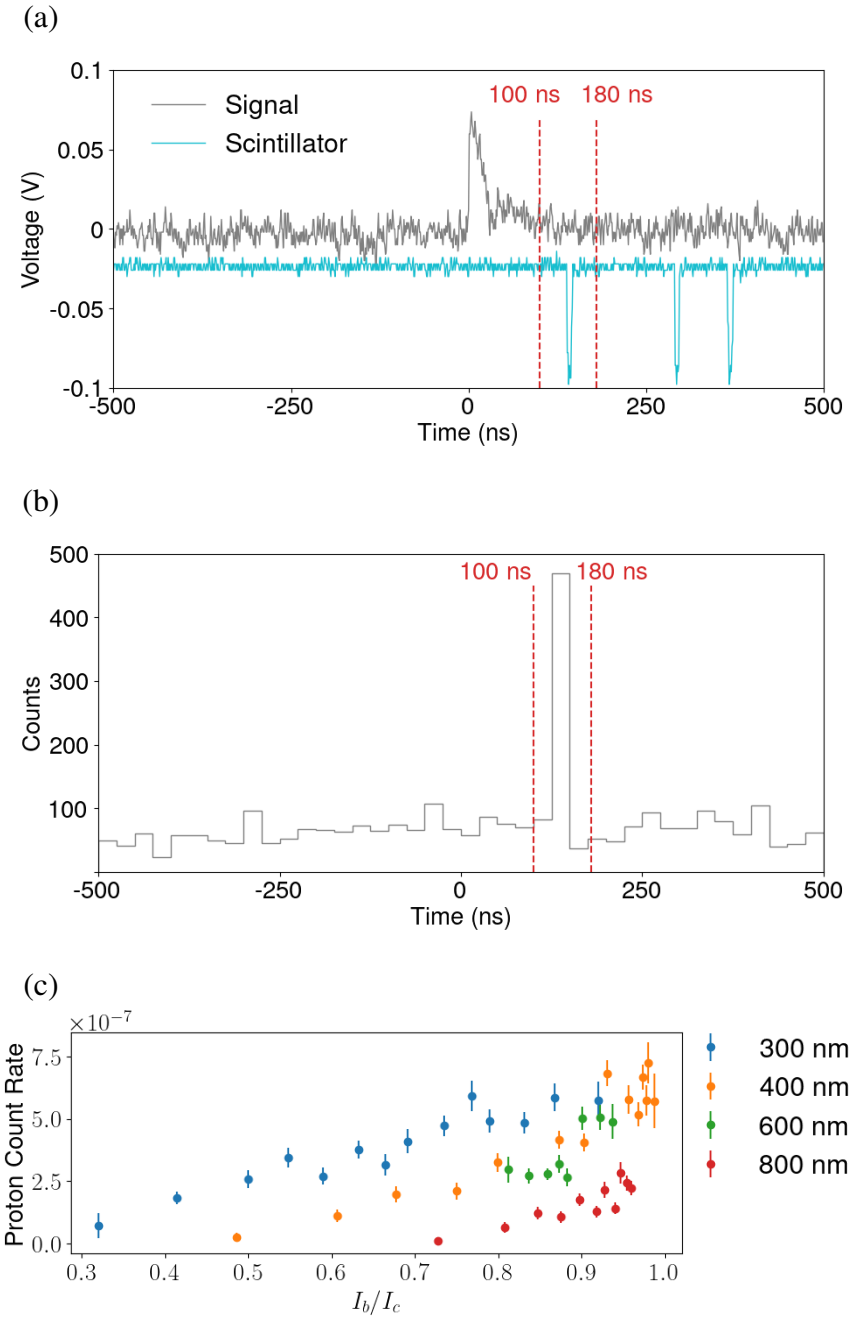

Figure 13: The preliminary beam test results at the FTBF. (a) A typical waveform from the nanowire (grey) and the plastic scintillator (cyan), (b) timing coincidence between the nanowire signal and the scintillator that defines the timing window of 100–180 ns delay, (c) the bias scan results with the vertical axis of proton count rate and the horizontal axis of the bias current normalized to the critical current of each device.

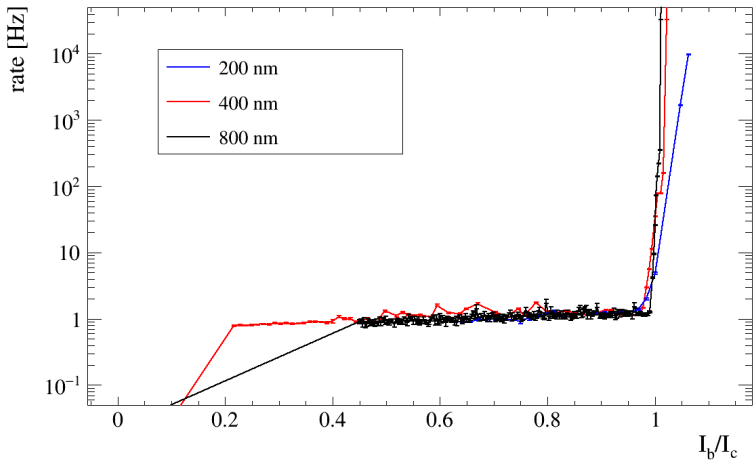

Figure 14: The preliminary results of the α detection test results at Argonne National Laboratory with ^{241}Am source.

similar to the FTBF setup (Figure 12) was installed at Argonne National Laboratory. Figure 14 shows the preliminary bias scan results for $200\,\mathrm{nm}$, $400\,\mathrm{nm}$ and $800\,\mathrm{nm}$ wide wires with α particles. In the case of proton detection in Figure 13, saturation of detection efficiency also occurs, but at lower I_b/I_c. One hypothesis is that the energy deposition of the α particle is large enough to create a hot spot at the lower bias current than in the proton case. Confirmation of this hypothesis by varying the wire geometry is ongoing. This suggests that the nanowire is capable of the auxiliary PID based on the design of the detector, the detection performance and the bias current setup.

4.3 Detection of Low Energy Electrons

Similar to the α detection (section 4.3), low-energy electron detection demonstrations are underway. 50 μCi industrial electron source arrived at Argonne National Laboratory in June 2023. Since then, engineering efforts have been made to improve the source holder and feedthrough to be ready for bias scan measurements.

4.4 Hardware Updates

Figure 12-b shows the current state of the nanowire and bias board, which provides stable bias current and serves as a test bed. We have made significant updates to the sensor design and fabrication process. Figure 15 shows the updated design of the wafers used for fabrication. We have gained access to the automated wire bonders used for the Imaging Calorimeter R&D (EICGENR&D2022 25) [64], which will facilitate detector assembly. The design report of the shift registers designed by the MIT group has recently been published [59] and will be tested in a similar testbed to the

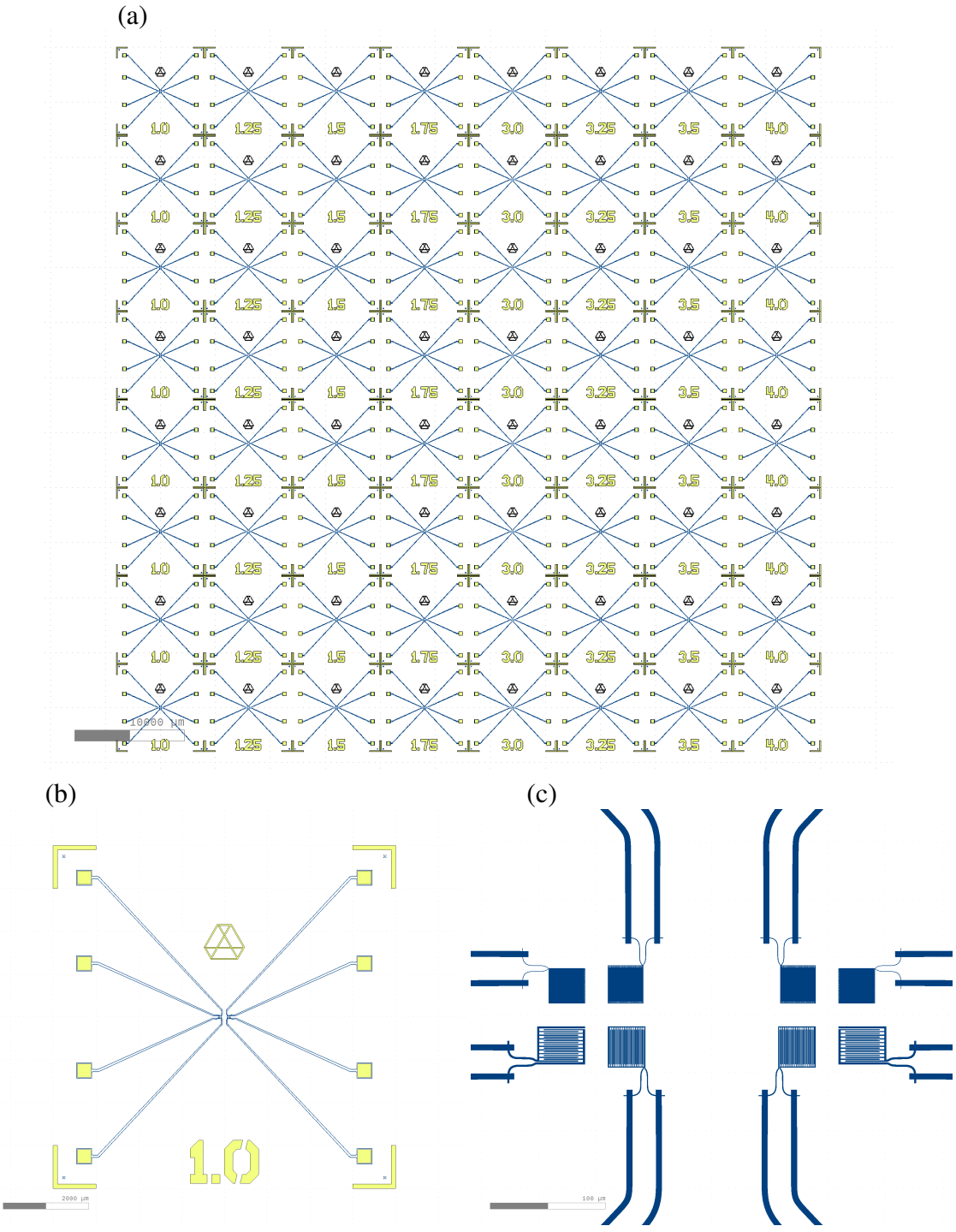

Figure 15: The updated nanowire wafer design for lithography that efficiently fabricates the sensors with different geometries. (a) Schematic drawing of the wafer array containing 64 devices with 8 different configurations. Each configuration has 8 negatively etched nanowires whose widths are multiples of 100, 200, 400, 800 nm. The multipliers are annotated on each device in yellow font. (b) A device with 100, 200, 400, 800 nm wide wires, where the multiplier is 1, (c) the magnified view of the wires in (b).

nanowire sensors.

4.5 Other Activities

- We held the HYDRA collaboration meeting from January 11, 2023 to January 13, 2023 to discuss the Co-Design process [65].
- We had invited talks at Workshop on Superconducting Electronics and Detectors (November 28, 2022–December 1, 2022) [66].
- We had a contributed talk at the 1st International Workshop on a 2nd Detector for the Electron-Ion Collider (May 17, 2023– May 19, 2023) [67].

5 Postdoctoral Fellows

Most postdoctoral fellows are affiliated with and fully funded by Argonne National Laboratory (ANL). Tomas Polakovic is a Maria Goeppert Mayer fellow at ANL. Sangbaek Lee is the ANL Medium Energy Group (MEP) postdoctoral fellow supported by the HYDRA collaboration. Marshall Schott and Shivangi Prasad are MEP postdoctoral fellows.

References

[1] GN Gol'Tsman, O Okunev, G Chulkova, A Lipatov, A Semenov, K Smirnov, B Voronov, A Dzardanov, C Williams, and Roman Sobolewski. Picosecond superconducting single-photon optical detector. *Applied physics letters*, 79(6):705–707, 2001.

[2] Junjie Wu, Lixing You, Sijing Chen, Hao Li, Yuhao He, Chaolin Lv, Zhen Wang, and Xiaoming Xie. Improving the timing jitter of a superconducting nanowire single-photon detection system. *Applied optics*, 56(8):2195–2200, 2017.

[3] F Marsili, Varun B Verma, Jeffrey A Stern, S Harrington, Adriana E Lita, Thomas Gerrits, Igor Vayshenker, Burm Baek, Matthew D Shaw, Richard P Mirin, et al. Detecting single infrared photons with 93% system efficiency. *Nature Photonics*, 7(3):210, 2013.

[4] WeiJun Zhang, LiXing You, Hao Li, Jia Huang, ChaoLin Lv, Lu Zhang, XiaoYu Liu, JunJie Wu, Zhen Wang, and XiaoMing Xie. Nbn superconducting nanowire single photon detector with efficiency over 90% at 1550 nm wavelength operational at compact cryocooler temperature. *Science China Physics, Mechanics & Astronomy*, 60(12):120314, 2017.

[5] Hiroyuki Shibata, Kaoru Shimizu, Hiroki Takesue, and Yasuhiro Tokura. Ultimate low system dark-count rate for superconducting nanowire single-photon detector. *Optics letters*, 40(14):3428–3431, 2015.

[6] Jiang Zhu, Yajun Chen, Labao Zhang, Xiaoqing Jia, Zhijun Feng, Ganhua Wu, Xiachao Yan, Jiquan Zhai, Yang Wu, Qi Chen, et al. Demonstration of measuring sea fog with an snspd-based lidar system. *Scientific reports*, 7(1):1–7, 2017.

[7] Hiroki Takesue, Shellee D Dyer, Martin J Stevens, Varun Verma, Richard P Mirin, and Sae Woo Nam. Quantum teleportation over 100 km of fiber using highly efficient superconducting nanowire single-photon detectors. *Optica*, 2(10):832–835, 2015.

[8] Hiroki Takesue, Sae Woo Nam, Qiang Zhang, Robert H Hadfield, Toshimori Honjo, Kiyoshi Tamaki, and Yoshihisa Yamamoto. Quantum key distribution over a 40-db channel loss using superconducting single-photon detectors. *Nature photonics*, 1(6):343, 2007.

[9] Jun Chen, Joseph B Altepeter, Milja Medic, Kim Fook Lee, Burc Gokden, Robert H Hadfield, Sae Woo Nam, and Prem Kumar. Demonstration of a quantum controlled-not gate in the telecommunications band. *Physical Review Letters*, 100(13):133603, 2008.

[10] Chandra M Natarajan, Michael G Tanner, and Robert H Hadfield. Superconducting nanowire single-photon detectors: physics and applications. *Superconductor science and technology*, 25(6):063001, 2012.

[11] A. Accardi et al. Electron Ion Collider: The Next QCD Frontier: Understanding the glue that binds us all. *Eur. Phys. J. A*, 52(9):268, 2016.

[12] R. Abdul Khalek et al. Science Requirements and Detector Concepts for the Electron-Ion Collider: EIC Yellow Report. 3 2021.

[13] National Academies of Sciences, Engineering, and Medicine. *An Assessment of U.S.-Based Electron-Ion Collider Science*. The National Academies Press, Washington, DC, 2018.

[14] E.C. Aschenauer, A.Tricoli, et al. A proposal for silicon detectors with high position and timing resolution as roman pots at eic, May 2019.

[15] A. V. Belitsky and A. V. Radyushkin. Unraveling hadron structure with generalized parton distributions. *Phys. Rept.*, 418:1–387, 2005.

[16] M. Hattawy et al. First Exclusive Measurement of Deeply Virtual Compton Scattering off ^{4}He: Toward the 3D Tomography of Nuclei. *Phys. Rev. Lett.*, 119(20):202004, 2017.

[17] Whitney Armstrong et al. Partonic Structure of Light Nuclei. *JLab PAC*, 2017.

[18] A. Dumitru, O. Evdokimov, A. Metz, C. Muñoz Camacho. YR Physics WG Conveners: overview and progress report. In *2nd EIC Yellow Report Workshop at Pavia University*, May 2020.

[19] AN Zotova and D Yu Vodolazov. Photon detection by current-carrying superconducting film: A time-dependent ginzburg-landau approach. *Physical Review B*, 85(2):024509, 2012.

[20] AD Semenov, RS Nebosis, Yu P Gousev, MA Heusinger, and KF Renk. Analysis of the nonequilibrium photoresponse of superconducting films to pulsed radiation by use of a two-temperature model. *Physical Review B*, 52(1):581, 1995.

[21] Alex D Semenov, Gregory N Gol'tsman, and Alexander A Korneev. Quantum detection by current carrying superconducting film. *Physica C: Superconductivity*, 351(4):349–356, 2001.

[22] Q Zhao, L Zhang, T Jia, L Kang, W Xu, J Chen, and P Wu. Intrinsic timing jitter of superconducting nanowire single-photon detectors. *Applied Physics B*, 104(3):673–678, 2011.

[23] Niccolò Calandri, Qing-Yuan Zhao, Di Zhu, Andrew Dane, and Karl K Berggren. Superconducting nanowire detector jitter limited by detector geometry. *Applied Physics Letters*, 109(15):152601, 2016.

[24] BA Korzh, Qing-Yuan Zhao, S Frasca, JP Allmaras, TM Autry, Eric A Bersin, M Colangelo, GM Crouch, AE Dane, T Gerrits, et al. Demonstrating sub-3 ps temporal resolution in a superconducting nanowire single-photon detector. *arXiv preprint arXiv:1804.06839*, 2018.

[25] M Biroth, P Achenbach, E Downie, and A Thomas. Silicon photomultiplier properties at cryogenic temperatures. *Nuclear Instruments and Methods in Physics Research Section A: Accelerators, Spectrometers, Detectors and Associated Equipment*, 787:68–71, 2015.

[26] Tomas Polakovic, Sergi Lendinez, John E. Pearson, Axel Hoffmann, Volodymyr Yefremenko, Clarence L. Chang, Whitney Armstrong, Kawtar Hafidi, Goran Karapetrov, and Valentine Novosad. Room temperature deposition of superconducting niobium nitride films by ion beam assisted sputtering. *APL Materials*, 6(7):076107, 2018.

[27] T. Polakovic, W.R. Armstrong, V. Yefremenko, J.E. Pearson, K. Hafidi, G. Karapetrov, Z.-E. Meziani, and V. Novosad. Superconducting nanowires as high-rate photon detectors in strong magnetic fields. *Nucl. Instrum. Meth. A*, 959:163543, 2020.

[28] Ilya Charaev, Alexey Semenov, Stefan Doerner, G Gomard, Konstantin Ilin, and Michael Siegel. Current dependence of the hot-spot response spectrum of superconducting single-photon detectors with different layouts. *Superconductor Science and Technology*, 30(2):025016, 2016.

[29] G Reffo, F Fabbri, K Wisshak, and F Käppeler. Fast neutron capture cross sections and related gamma-ray spectra of niobium-93, rhodium-103, and tantalum-181. *Nuclear Science and Engineering*, 80(4):630–647, 1982.

[30] AB Smith, PT Guenther, and JF Whalen. Neutron total and scattering cross sections of niobium in the continuum region. *Zeitschrift für Physik*, 264(5):379–398, 1973.

[31] SP Chockalingam, Madhavi Chand, Anand Kamlapure, John Jesudasan, Archana Mishra, Vikram Tripathi, and Pratap Raychaudhuri. Tunneling studies in a homogeneously disordered s-wave superconductor: Nbn. *Physical Review B*, 79(9):094509, 2009.

[32] E Piatti, A Sola, D Daghero, GA Ummarino, F Laviano, JR Nair, C Gerbaldi, R Cristiano, A Casaburi, and RS Gonnelli. Superconducting transition temperature modulation in nbn via edl gating. *Journal of Superconductivity and Novel Magnetism*, 29(3):587–591, 2016.

[33] NK Sherman. Superconducting nuclear particle detector. *Physical Review Letters*, 8(11):438, 1962.

[34] Nobuyuki Zen, Yigang Chen, Koji Suzuki, Masataka Ohkubo, Shigehito Miki, and Zhen Wang. Development of superconducting strip line detectors (sslds) for time-of-flight mass spectrometers (tof-ms). *IEEE transactions on applied superconductivity*, 19(3):354–357, 2009.

[35] A Casaburi, E Esposito, M Ejrnaes, K Suzuki, M Ohkubo, S Pagano, and R Cristiano. A 2×2 mm2 superconducting strip-line detector for high-performance time-of-flight mass spectrometry. *Superconductor Science and Technology*, 25(11):115004, 2012.

[36] M Ohkubo. Superconducting detectors for particles from atoms to proteins. *Physica C: Superconductivity*, 468(15-20):1987–1991, 2008.

[37] K Suzuki, S Miki, S Shiki, Y Kobayashi, K Chiba, Z Wang, and M Ohkubo. Ultrafast ion detection by superconducting nbn thin-film nanowire detectors for time-of-flight mass spectrometry. *Physica C: Superconductivity*, 468(15-20):2001–2003, 2008.

[38] Kyosuke Sano, Yoshihiro Takahashi, Yuki Yamanashi, Nobuyuki Yoshikawa, Nobuyuki Zen, and Masataka Ohkubo. Demonstration of single-flux-quantum readout circuits for time-of-flight mass spectrometry systems using superconducting strip ion detectors. *Superconductor Science and Technology*, 28(7):074003, 2015.

[39] Koji Suzuki, Shigetomo Shiki, Masahiro Ukibe, Masaki Koike, Shigehito Miki, Zhen Wang, and Masataka Ohkubo. Hot-spot detection model in superconducting nano-stripline detector for kev ions. *Applied physics express*, 4(8):083101, 2011.

[40] Hatim Azzouz, Sander N Dorenbos, Daniel De Vries, Esteban Bermúdez Ureña, and Valery Zwiller. Efficient single particle detection with a superconducting nanowire. *AIP Advances*, 2(3):032124, 2012.

[41] Alex Malins, Masahiko Machida, The Dang Vu, Kazuya Aizawa, and Takekazu Ishida. Monte carlo radiation transport modelling of the current-biased kinetic inductance detector. *Nuclear Instruments and Methods in Physics Research Section A: Accelerators, Spectrometers, Detectors and Associated Equipment*, 953:163130, 2020.

[42] Yuki Iizawa, Hiroaki Shishido, Kazuma Nishimura, Kenji M Kojima, Tomio Koyama, Kenichi Oikawa, Masahide Harada, Shigeyuki Miyajima, Mutsuo Hidaka, Takayuki Oku, et al. Energy-resolved neutron imaging with high spatial resolution using a superconducting delay-line kinetic inductance detector. *Superconductor Science and Technology*, 32(12):125009, 2019.

[43] Hiroaki Shishido, Yuya Miki, Hiroyuki Yamaguchi, Yuki Iizawa, Kenji M Kojima, Tomio Koyama, Kenichi Oikawa, Masahide Harada, Shigeyuki Miyajima, Mutsuo Hidaka, et al. High-speed neutron imaging using a current-biased delay-line detector of kinetic inductance. *Physical Review Applied*, 10(4):044044, 2018.

[44] Naohito Yoshioka, Ikutaro Yagi, Hiroaki Shishido, Tsutomu Yotsuya, Shigeyuki Miyajima, Akira Fujimaki, Shigehito Miki, Zhen Wang, and Takekazu Ishida. Current-biased kinetic inductance detector using mgb_2 nanowires for detecting neutrons. *IEEE transactions on applied superconductivity*, 23(3):2400604–2400604, 2013.

[45] I. D. Conway Lamb, J. I. Colless, J. M. Hornibrook, S. J. Pauka, S. J. Waddy, M. K. Frechtling, and D. J. Reilly. An fpga-based instrumentation platform for use at deep cryogenic temperatures. *Review of Scientific Instruments*, 87(1):014701, 2016.

[46] M. S. Allman, V. B. Verma, M. Stevens, T. Gerrits, R. D. Horansky, A. E. Lita, F. Marsili, A. Beyer, M. D. Shaw, D. Kumor, R. Mirin, and S. W. Nam. A near-infrared 64-pixel superconducting nanowire single photon detector array with integrated multiplexed readout. *Applied Physics Letters*, 106(19):192601, 2015.

[47] Emma E. Wollman, Varun B. Verma, Adriana E. Lita, William H. Farr, Matthew D. Shaw, Richard P. Mirin, and Sae Woo Nam. Kilopixel array of superconducting nanowire single-photon detectors. *Opt. Express*, 27(24):35279–35289, Nov 2019.

[48] A. Arno et al. Eic deisgn study, 2019.

[49] Yuji Goto et al. Development of position sensitive zero degree calorimeter for eic, January 2020.

[50] R.L. Witkover, R.J. Michnoff, and J.M. Geller. Rhic beam loss monitor system initial operation. In *Proceedings of the 1999 Particle Accelerator Conference (Cat. No.99CH36366)*, volume 3, pages 2247–2249 vol.3, 1999.

[51] Jianxun Yan, Trent Allison, Scott Bruhwel, and Weiwei Lu. Signal Processing for Beam Loss Monitor System at Jefferson Lab. In *7th International Beam Instrumentation Conference*, page TUPA16, 2019.

[52] EIC Detector Advisory Committee. Report of the 19th Electron Ion Collider Detector R&D Meeting, 7 2020.

[53] Braga, Davide. SNSPD cold readout: activities and plans, July 2022.

[54] Adam N. McCaughan and Karl K. Berggren. A superconducting-nanowire three-terminal electrothermal device. *Nano Letters*, 14(10):5748–5753, 2014. PMID: 25233488.

[55] Adam N. McCaughan, Nathnael S. Abebe, Qing-Yuan Zhao, and Karl K. Berggren. Using Geometry To Sense Current. *Nano Letters*, 16(12):7626–7631, December 2016. Publisher: American Chemical Society.

[56] Qing-Yuan Zhao, Emily A. Toomey, Brenden A. Butters, Adam N. McCaughan, Andrew E. Dane, Sae-Woo Nam, and Karl K. Berggren. A compact superconducting nanowire memory element operated by nanowire cryotrons. *Superconductor Science and Technology*, 31(3):035009, February 2018. Publisher: IOP Publishing.

[57] Reza Baghdadi, Jason P. Allmaras, Brenden A. Butters, Andrew E. Dane, Saleem Iqbal, Adam N. McCaughan, Emily A. Toomey, Qing-Yuan Zhao, Alexander G. Kozorezov, and Karl K. Berggren. Multilayered Heater Nanocryotron: A Superconducting-Nanowire-Based Thermal Switch. *Physical Review Applied*, 14(5):054011, November 2020. Publisher: American Physical Society.

[58] EIC Detector Advisory Committee. Report of the 20th Electron Ion Collider Detector R&D Meeting, 3 2021.

[59] Reed A. Foster, Matteo Castellani, Alessandro Buzzi, Owen Medeiros, Marco Colangelo, and Karl K. Berggren. A superconducting nanowire binary shift register. *Applied Physics Letters*, 122(15):152601, 04 2023.

[60] Alessandro Buzzi. Building Blocks Design for Superconducting Nanowire Asynchronous Logic, 2022.

[61] Qing-Yuan Zhao, Emily A. Toomey, Brenden A. Butters, Adam N. McCaughan, Andrew E. Dane, Sae-Woo Nam, and Karl K. Berggren. A compact superconducting nanowire memory element operated by nanowire cryotrons. *Superconductor Science Technology*, 31(3):035009, July 2018.

[62] Whitney Armstrong et al. Superconducting Nanowire Detectors for the EIC, EIC-Related Generic Detector R&D Program (2022), EICGENR&D2022 18, https://www.jlab.org/sites/default/files/eic_rd_prgm/files/2022_Proposals/EIC_nanowires_July2022_EICGENRandD2022_18.pdf.

[63] Howard C. Fenker. A Standard Beam PWC for Fermilab, FERMILAB-TM-1179. Feb. 1983.

[64] Maria Żurek et al. Imaging Calorimetry for the Electron-Ion Collider, EIC-Related Generic Detector R&D Program (2022), EICGENR&D2022 25, https://www.jlab.org/sites/default/files/eic_rd_prgm/files/2022_Proposals/EIC_R_D_Imaging_Calo_EICGENRandD2022_25.pdf.

[65] Fermilab Newsroom. HYDRA Collaboration Meeting, https://news.fnal.gov/2023/07/fermilab-led-microelectronics-codesign-team-works-to-develop-a-cutting-edge-particle-detector/.

[66] Whitney Armstrong et al. *Applications of Superconducting Electronics and Detectors Workshop* (2022), https://indico.jlab.org/event/555/.

[67] Whitney Armstrong. Nanowire, *1st International Workshop on a 2nd Detector for the Electron-Ion Collider* (2023), https://indico.bnl.gov/event/18414/contributions/.